Liquid Crystals
Publication details, including instructions for authors and subscription information:
http://www.informaworld.com/smpp/title~content=t713926090

Angular and frequency dependent spin relaxation study of liquid crystalline cyanobiphenyls

J. Struppe[a]; F. Noack[a]
[a] Physikalisches Institut Teil 4 der Universität Stuttgart, Stuttgart, Germany

To cite this Article Struppe, J. and Noack, F.(1996) 'Angular and frequency dependent spin relaxation study of liquid crystalline cyanobiphenyls', Liquid Crystals, 20: 5, 595 — 606
To link to this Article: DOI: 10.1080/02678299608031148
URL: http://dx.doi.org/10.1080/02678299608031148

LIQUID CRYSTALS, 1996, VOL. 20, NO. 5, 595-606

Angular and frequency dependent spin relaxation study of liquid crystalline cyanobiphenyls

by J. STRUPPE and F. NOACK*
Physikalisches Institut Teil 4 der Universität Stuttgart, 70550 Stuttgart, Germany

(*Received 27 March 1995; in final form 10 July 1995; accepted 21 October 1995*)

NMR field-cycling measurements of the Larmor frequency (ν) and angular (Δ) dependences of the longitudinal proton spin relaxation time T_1 for the nematic liquid crystals 5CB and 8CB allow a more detailed analysis of the underlying molecular motions than data available previously. All $T_1(\nu, \Delta)$ dispersion profiles essentially distinguish three frequency ranges where T_1 is governed by either local field effects, collective motions (director order fluctuations), or rotational and translational diffusion of individual molecules or molecular groups, respectively. The angular dependence supports and extends previous conclusions about the significance of the order fluctuation term at low (kHz) and high (MHz) Larmor frequencies; in addition it is the basis for the disentanglement of local field effects, which involve Jeener's dipolar relaxation, and of the sophisticated rotational relaxation models suggested in the literature by Dong, Nordio and Vold. It is found that Vold's third rate concept gives the best explanation of the measurements. The results on the rotational diffusion processes essentially agree with deuteron studies from the literature, but also reveal clear distinctions with regard to the anisotropy parameter σ, essentially due to the improved separation from the order fluctuation contribution.

1. Introduction

NMR spin relaxation measurements of liquid crystals (LCs) provide rather detailed information about molecular motions like anisotropic rotational and translational diffusion processes of single molecules, and in particular about a peculiar feature of liquid crystalline phases, namely *collective molecular motions* or order fluctuations [1-3]. However, the discrimination of these contributions to the observed total relaxation rate, and even more the distinction of effects coming from individual segments of the non-rigid molecules, is not straightforward, so that satisfactory results are only available for very few selected systems such as some azoxybenzenes and cyanobiphenyls. Up to the present, the most helpful means of performing a reliable analysis of the various superimposed relaxation mechanisms contributing to the overall magnetic resonance signal have been found to be:

(a) to study both the longitudinal Zeeman *proton* and *deuteron* relaxation times T_1 in selectively deuteriated molecules [1-3];
(b) to combine T_1 with dipolar and quadrupolar (T_{1D}, T_{1Q}) relaxation experiments using the Jeener-Broekaert pulse sequence [1-4];
(c) to observe the Larmor frequency dependence $T_1(\nu)$(dispersion) of proton and deuteron relaxation times over a broad range by suitable field-cycling techniques [2, 5, 6].

* Author for correspondence.

A means difficult to realize for reasons shown below and hence relatively seldom used to improve the relaxation model analysis is to consider directly the anisotropy of the underlying molecular reorientations by observing the angular dependent spin relaxation of the liquid crystal. As recently pointed out once more by Morrison *et al.* [7], such a step considerably enriches the amount of experimental data in order better to discriminate alternative models. This paper presents an extensive study of both the *frequency* and *angular* dependence of the proton spin relaxation time T_1 for two nematogenic liquid crystals (cyanobiphenyls), making use of more powerful angular dependent field-cycling methods than were available previously [8-10].

2. Experimental techniques

Measurements of the angular dependence of nuclear spin relaxation times in low-viscosity nematic liquid crystals, i.e. for different orientations of the nematic director $\mathbf{n}$ relative to the external Zeeman field $\mathbf{B}_0$, are difficult because normally $\mathbf{n}$ aligns rather fast parallel to $\mathbf{B}_0$ (if the anisotropy of the magnetic susceptibility is positive as usual), and hence the mechanical rotation of the director by a desired angle is generally too slow to obtain a well defined quasi-stationary state with $\mathbf{n}$ oblique to $\mathbf{B}_0$. To overcome this difficulty, several methods have been described in the literature [11-13]: namely the spinning of the sample with adequate speed about an axis perpendicular to $\mathbf{B}_0$ [11], the superposition of the Zeeman field

0267-8292/96 $12·00

by a strong electric field to incline the director against $\mathbf{B}_0$ [12], or the fast switching of the magnetic field direction [13]. All three procedures involve problems, because the director field may become inhomogeneous through electric conductivity or flow effects. However, such perturbations can be most transparently controlled by the field switching technique [10, 13].

In extension of previous work using fast field-cycling techniques to adjust a selectable angle Δ between $\mathbf{n}$ and $\mathbf{B}_0$ [8–10], we have developed a more powerful device which allows angular dependent spin relaxation measurements over a broader Larmor frequency range. The principle of the method is the following (figure 1): in order to rotate the $\mathbf{B}_0$ field from the initial orientation parallel to the director to another angle and magnitude, the field-cycling method must be applied to two magnet coils with their fields orthogonal to each other, e.g. parallel to the laboratory z- and x-axes, respectively. Switching the relative magnitudes of the two fields B_z and B_x rotates the total field from initially $\mathbf{B}_0 \equiv \mathbf{B}_z$ to

$$\mathbf{B}_\Delta = B_x \mathbf{e}_x + B_z \mathbf{e}_z \qquad (1\,a)$$

by an adjustable angle

$$\Delta = \arctan\left(\frac{B_x}{B_z}\right), \quad 0 \leqslant \Delta \leqslant 90^\circ \qquad (1\,b)$$

depending on the value of the components B_x and B_z. The Larmor frequency adjustable by the field-cycling technique in addition to the angle is

$$\nu = \frac{\gamma}{2\pi} B_\Delta, \qquad (1\,c)$$

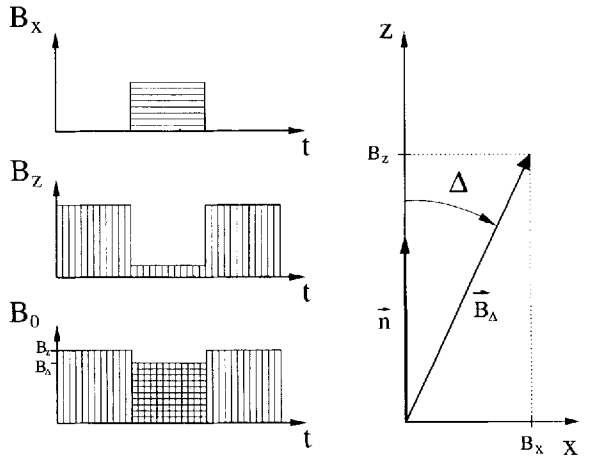

Figure 1. Principle of the fast field-cycling NMR method for angular and frequency dependent relaxation time measurements, where the orientation and strength of the total Zeeman field $\mathbf{B}_\Delta$ are cycled periodically by means of two perpendicular fields B_x and B_z relative to a selected axis, which in this case is the liquid crystal director $\mathbf{n}$.

where γ is the gyromagnetic ratio of the examined spins. Originally, we achieved the field rotation by mounting a pair of Helmholtz coils *outside* the B_z field cyclinder coil with its axes perpendicular to the B_z magnet axis [8]. Using a total available electrical power of 28 kW, together with a power splitting device to drive both the main magnet ($B_{z\,\max} = 0{\cdot}16$ T, corresponding to a proton Larmor frequency $\nu_{\max} = 6{\cdot}8$ MHz) and the additional Helmholtz pair, we previously obtained a maximum field $B_{x\,\max} = 0{\cdot}047$ T [8] (which allowed $\Delta = 90^\circ$ adjustments up to $\nu = 2$ MHz). However, such a geometry proved rather ineffective for work at still higher fields B_Δ, because it needs too much power for a desired magnetic field rotation. Our more recent field-cycling concept makes use of smaller, optimized cylindrical magnet geometries which provide much stronger B_z fields with less electric power [14]. Following this concept, we combined one of our present B_z coils [10] ($B_{z\,\max} = 0{\cdot}21$ T, $\nu_{\max} = 8{\cdot}9$ MHz) with an additional saddle coil [15, 16] *inside* the cylinder bore to get the switchable perpendicular field B_x.

To provide a strong field B_x at the probe, it is necessary to keep the effective volume of the auxiliary magnet small, to make the inductance as large as compatible with the desired switching time [10], and to maximize the allowed current according to the approximate field relations [10]

$$(B_x)_{\max} \cong \left(\frac{\mu L}{V_{\text{eff}}}\right)^{1/2} I_{\max}, \qquad (2\,a)$$

$$\left(\frac{\mathrm{d}B_x}{\mathrm{d}t}\right)_{\max} \cong \left(\frac{\mu}{L V_{\text{eff}}}\right)^{1/2} U_{\max} \qquad (2\,b)$$

where L is the coil inductance, V_{eff} the effective field volume, μ the magnetic permeability in the bore, $I_{\max}$ the current through the wire, and $U_{\max}$ the driving voltage. Since the value of L is rather small in the present case, equation (2 *a*) is the critical one. In order to reduce the field volume, we looked for a possibility of mounting the B_x magnet *inside* the bore of our main B_z magnet (figure 2). A suitable choice for that purpose is a saddle coil [15, 16]. Since the inductance increases for higher numbers N of the windings, N should be as large as possible in the available space. This number was restricted on the one hand by the available cylindrical cross-section (diameter = 36 mm) of the glass tube which separates the cooling circuits of both magnets and by the outer diameter (24·5 mm) of the sample dewar, and on the other hand by the increasing resistance of the coil which is proportional to the conductor length for a given cross-section of the wire. To get a sufficient homogeneity of $B/\Delta B > 10^2$ over the sample, the length of the saddle coil had to be chosen as 10 cm [15]. The best field-to-power

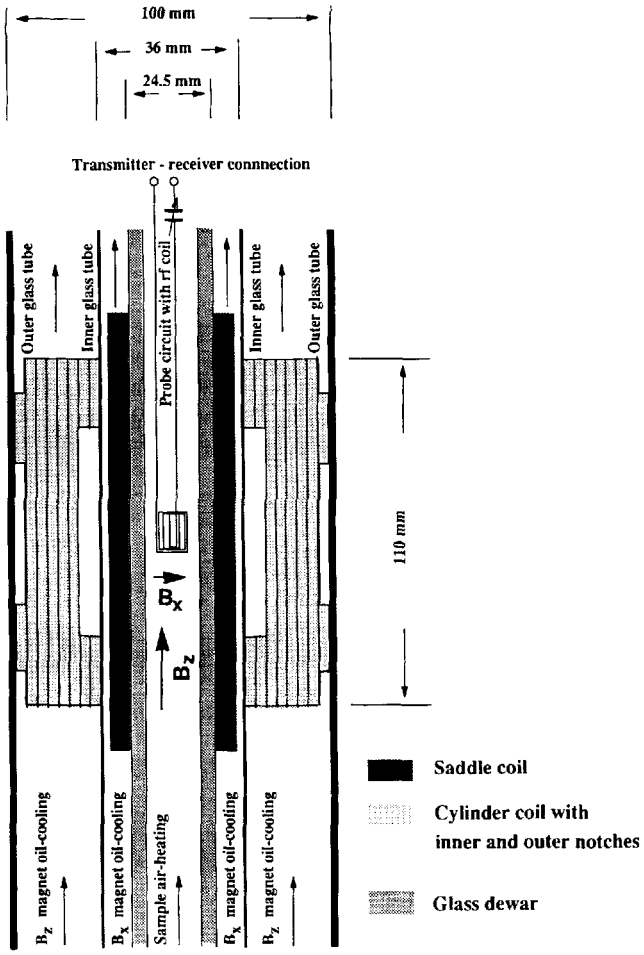

Figure 2. Schematic geometry and cooling circuits of the air-cored cylinder coil (B_z) and saddle coil (B_x) combination for fast switching of both the orientation and strength of the NMR Zeeman field up to $B_\Delta = 0{\cdot}21$ T. The achievable transit times are described in the text.

ratio of this prototype magnet, matched to a commercial switchable 1 kW power supply (Heinzinger TN 100/10, 100 V, 10 A), was found by calculating the resistance R_s of the coil at the estimated working temperature of 100 to 170°C. At these temperatures, realized by an oil cooling circuit separated from that of the main magnet, R_s increases by a factor between 1·3 to 1·6 compared with the copper resistance measured at room temperature. Further, being restricted to commercially obtainable copper conductors, we had to look for a favourable compromise between voltage or current mismatch. The best choice proved to be a wire with 0·5 mm diameter which, using 160 windings, gave a resistance of 4·5 Ω at room temperature and 6 Ω at the working temperature. This prototype magnet produces a field of $B_x = 0{\cdot}044$ T ($\nu \approx 1{\cdot}87$ MHz) with the maximum available current of 11 A. By increasing the power from 1 to 3 kW (Delta Electronika SM 120/25, 125 V, 25 A), changing the saddle coil geometry somewhat for a larger wire diameter (0·7 mm) and slightly reducing the outer sample dewar diameter (21·5 mm), we are going to strengthen the maximum field to $B_x = 0{\cdot}14$ T. With the presently operating network, i.e. the prototype saddle coil and the 3 kW power supply, it is already possible to perform angular dependent proton T_1 measurements at an angle $\Delta = 90°$ up to $\nu = 4{\cdot}5$ MHz, whereas the new saddle coil will extend the range for $\Delta = 90°$ up to $\nu = 6$ MHz and for $\Delta = 42{\cdot}4°$ up to 8·9 MHz.

For higher Larmor frequencies, i.e. above the instrumental limitations described before, the angular dependence of T_1 in LCs could still be measured by a mechanical rotation of the LC with fixed oriented molecules as a result of confinement effects [17, 18]. This was achieved by filling the LC into anopore membranes. Such materials form macroscopically aligned honeycomb channels with approximately 0·2 μm diameter in which the LC orients uniformly parallel to the channel axes, even in high magnetic fields up to 4·7 T [18]. We could show [19] by comparison of both techniques at Larmor frequencies between $\nu \cong 4{\cdot}5$ MHz and 5 kHz, over the range where both methods work, that the anopore alignment gives the same results as the angular adjustment by field-cycling.

The sample materials, 4-pentyl-4′-cyanobiphenyl (5CB) and 4-octyl-4′-cyanobiphenyl (8CB), were purchased from Merck Ltd, UK and sealed without further purification after degassing by the usual freeze-thaw method under vacuum. The 5CB anopore membrane sample was kindly prepared by H. Schmiedel as described elsewhere [18].

3. Results

Figure 3 shows details of the angular dependent field-cycling T_1 sequence. In the first period I, the magnetization M with the director orientation of the liquid crystalline sample parallel to the polarization field B_z is created. In the following period II, after rotating B_z to B_Δ, the magnetization M exponentially decays with the time constant $T_1(\nu, \Delta)$ in the relaxation field B_Δ at the orientation Δ, e.g. Δ_1 or Δ_2, relative to the director **n**. This decay is measured in period III as a function of $|\mathbf{B}_\Delta|$ ($\hat{=} \nu$) and Δ by the FID signal U_{sig} following the $\pi/2$ rf B_1-pulse after the field is switched back to a magnitude of B_z which fulfils the resonance condition of the probe circuit ($\nu = 8{\cdot}9$ MHz).

Figures 4 and 5 illustrate selected results of our $T_1(\nu, \Delta)$ measurements for 5CB and 8CB, respectively, namely the proton T_1 relaxation dispersion $T_1(\nu)$ at different director orientations Δ (figure 4), and the related angular dependence $T_1(\Delta)$ at selected Larmor

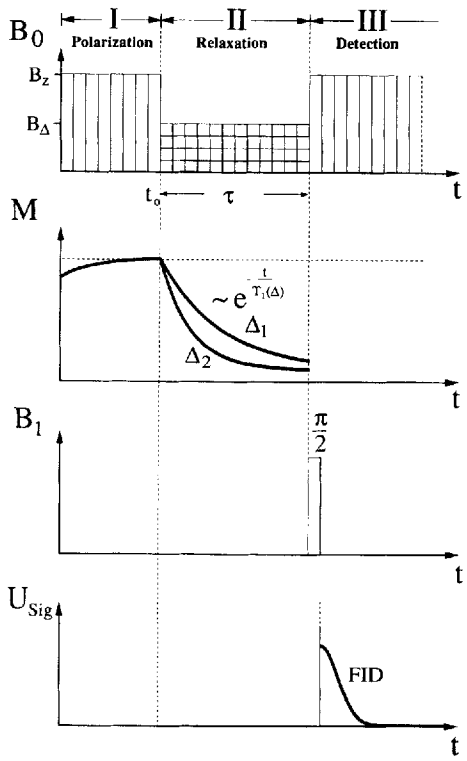

Figure 3. Polarization, relaxation and detection periods (I, II, III) of the fast field-cycling experiment used for $T_1(\nu, \Delta)$ measurements of liquid crystals, showing schematically two magnetization decays $M(t)$ in period II at different angles Δ. The signal U_{sig} is sampled by means of a $\pi/2$ rf-field irradiation pulse $B_1(t)$ by the amplitude of the free induction decay (FID), excited at the beginning of period III.

frequencies ν (figure 5). The measurements were performed in the middle of the nematic temperature ranges (30°C, 37°C) and exhibit the following characteristic features:

(a) The relaxation dispersion shows at both orientations ($\Delta = 0°$, $\Delta = 90°$) the form typical for nematics [5], i.e. (i) the low frequency square-root regime $T_1 \sim \nu^{1/2}$ ($\nu \leqslant 10^6$ Hz) with a plateau below $\nu \approx 10^4$ Hz at $\Delta = 0$ and a minimum at $\Delta = 90°$; (ii) the medium frequency range ($10^6 \leqslant \nu \leqslant 10^7$ Hz) where $T_1(\nu)$ approaches a high frequency plateau; (iii) the high frequency range ($\nu \geqslant 10^7$ Hz) with a shallow but increasing $T_1(\nu)$ slope.

(b) For $\nu \geqslant 20$ kHz the dispersion profiles are similar for both orientations, but the angular dependence decreases slightly with increasing Larmor frequency from a factor of 2 in range (i) above $\nu \approx 20$ kHz to a factor of 1·3 in range (iii). For $\nu \leqslant 20$ kHz where the $T_1(\nu)$ minimum occurs, the ratio $T_1(\Delta = 0°)/T(\Delta = 90°)$ becomes much larger than 2, namely up to $5 \pm 30\%$. This is also demonstrated by figure 5, which presents the full angular dependence between $\Delta = 0°$ and 90° at 2, 50 and 500 kHz for both materials, and for 5CB also at 10 kHz and 28 MHz.

(c) The $T_1(\nu, \Delta)$ plots are almost identical for both 5CB and 8CB but the relaxation times are somewhat shorter in the second case.

As estimated from the root-mean square error of control measurements, the accuracy of the T_1 data shown is $\pm 10\%$ for $\nu < 10$ kHz and $\pm 5\%$ for $\nu > 10$ kHz in the case of the LC bulk samples. This error is slightly higher in the case of the anopore confinement, namely $\pm 20\%$ and $\pm 10\%$, respectively, because the amount of LC material in the anopore membranes was only one quarter (0·2 g) of that in the bulk sample (0·8 g); it is also $\pm 20\%$ for the angular dependent data of all samples in the range of the minimum.

4. Theory and discussion

4.1. *General theory*

Nematic liquid crystals are systems which usually exhibit cylindrical symmetry about the nematic director **n** [1–3]. For such systems, the orientation dependence of the spin relaxation for any desired angle Δ between the Zeeman field $\mathbf{B}_\Delta$ and the director **n** can be obtained by a model independent transformation [1–3, 20] of the motional spectral densities calculated for one special angle, e.g. for $\Delta = 0$. Up to the present, most of the

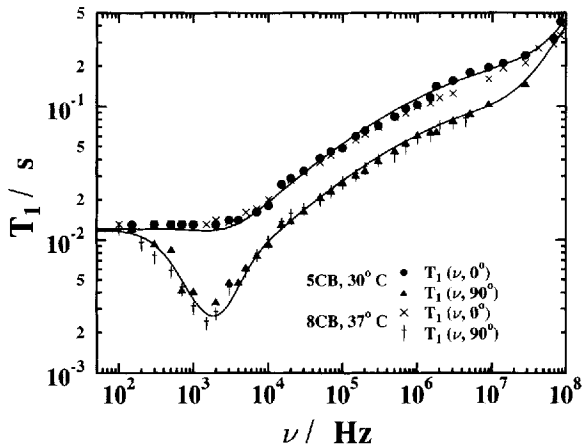

Figure 4. Larmor frequency dependence of the longitudinal proton spin relaxation time T_1 of 5CB and 8CB, respectively, for two orientations Δ between the nematic director **n** and the Zeeman field $\mathbf{B}_\Delta$, at temperatures approximately in the middle of the mesophase ranges (30°C, 37°C). The diagram distinguishes at least three characteristic relaxation regimes. The full lines are model fits to the 5CB data (for details see text and figure 6). On average, T_1 of 5CB is identical or slightly longer than T_1 of 8CB.

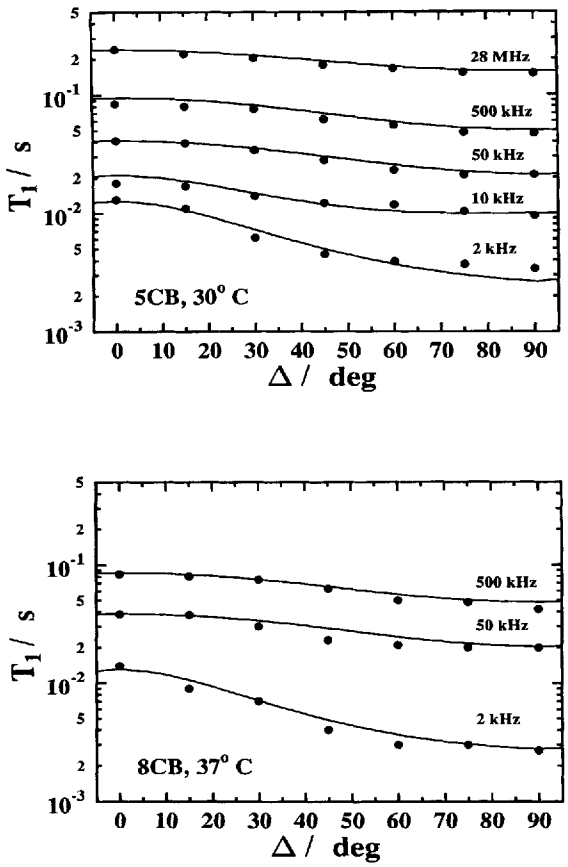

Figure 5. Angular dependence of the longitudinal proton spin relaxation time T_1 of 5CB (top) and 8CB (bottom) at different Larmor frequencies ν to illustrate the characteristic $T_1(\Delta)$ changes between the three $T_1(\nu)$ regimes. The full lines are model simulations of the experimental data points with the parameters listed in table 2. On average, T_1 of 5CB at $\Delta=0°$ is slightly longer than T_1 of 8CB, but the difference disappears for larger angles Δ.

calculations reported in the literature are primarily concerned with the relaxation of deuteron (^{2}H) spins, because deuterons allow one to separate different spin positions on the molecules. This is not the case for protons (^{1}H), which means that in order to use the relaxation models for protons, the relaxation rates have to be averaged over many proton sites to allow an analysis of the experimental data. On the other hand, presently it is not yet possible to perform angular dependent field-cycling measurements with deuterons as with protons, because of instrumental limitations. The necessary averaging procedure is briefly described below. It implies that the LCs considered show a mono-exponential proton magnetization decay due to fast spin exchange between unlike positions.

Assuming for simplicity the case of *fast* magnetization exchange between different kinds of dipolar coupled, inter- and intramolecular proton pairs i,k (e.g. phenyl or alkyl positions), and making use of standard high-field relaxation expressions (Zeeman-field B_Δ larger than local dipolar field B_{loc}) for different types of molecular reorientations M of such pairs (e.g. collective or individual motions), gives for the Larmor frequency (ν), and angular (Δ) dependence of the averaged, total proton Zeeman relaxation rate [21] parallel (longitudinal) to the sufficiently large external Zeeman field B_Δ

$$T_{1Z}^{-1}(\nu,\Delta)\equiv R_{1Z}=\sum_M R_{1M}, \tag{3}$$

where the relaxation rate R_{1M} of one single process M can be written in terms of two spectral densities $J_M^{(p)}(p\nu,\Delta)$ with $p=1,2$ in the standard form for $I=1/2$ spins [1-3, 20]

$$R_{1M}(\nu,\Delta)=\frac{9}{8}\left(\frac{\mu_0\gamma^2\hbar}{4\pi}\right)^2[J_M^{(1)}(\nu,\Delta)+J_M^{(2)}(2\nu,\Delta)], \tag{4}$$

with ν given by equation (1 *c*). In equations (3) and (4) μ_0, γ, and $\hbar$, denote the magnetic vacuum permeability, the gyromagnetic ratio of protons, and Planck's constant divided by 2π, respectively. The two angular dependent spectral densities $J_M^{(p)}(p\nu,\Delta)$, $p=1,2$, are obtained from three spectral densities $J_M^{(q)}(p\nu,\Delta=0°)$, $q=0,1,2$, at the particular orientation $\Delta=0°$ (in the following we will omit writing the angle, if $\Delta=0°$) by

$$J_M^{(p)}(p\nu,\Delta)=\sum_q F_{pq}(\Delta)J_M^{(q)}(p\nu,\Delta=0°)\equiv\sum_q F_{pq}(\Delta)J_M^{(q)}(p\nu); \tag{5}$$

via the transformation matrix $F_{pq}(\Delta)$ [1, 20]. Explicitly this means in equation (4) the angular dependences

$$\begin{aligned}J_M^{(1)}(\nu,\Delta)=&\tfrac{1}{4}\cos^2(\Delta)\sin^2(\Delta)\,J_M^{(0)}(\nu)\\&+\tfrac{1}{2}(1-3\cos^2(\Delta)+4\cos^4(\Delta))\,J_M^{(1)}(\nu)\\&+\tfrac{1}{8}(1-\cos^4(\Delta))\,J_M^{(2)}(\nu)\end{aligned} \tag{6a}$$

and

$$\begin{aligned}J_M^{(2)}(2\nu,\Delta)=&\tfrac{1}{4}\sin^4(\Delta)\,J_M^{(0)}(2\nu)\\&+2(1-\cos^4(\Delta))\,J_M^{(1)}(2\nu)\\&+\tfrac{1}{8}(1+6\cos^2(\Delta)+\cos^4(\Delta))\,J_M^{(2)}(2\nu),\end{aligned} \tag{6b}$$

respectively. As can be seen from equation (6), $T_1(\Delta)$ differs for unlike M if the ratios $J_M^{(0)}:J_M^{(1)}:J_M^{(2)}$ are not the same for the considered motions. The special forms of the spectral densities $J_M^{(q)}(p\nu)$ used to discuss the measurements of this paper are taken from the literature with some necessary numerical modifications, and are summarized in the Appendix.

Somewhat differently from *deuteron* relaxation studies, frequency dependent *proton* measurements of liquid crystals have shown significant effects of at least

three kinds of mechanisms M, namely: **O**rder director **f**luctuation (OF), **rot**ational diffusion (ROT) and translational **s**elf-**d**iffusion (SD), which are essentially distinguished by their characteristic $T_1(\nu)$ profiles [5]. (The significance of cross-terms has never been demonstrated clearly, and quadrupolar cross-relaxation effects have not been observed reliably in non-deuteriated 5CB and 8CB [6, 19].) By the T_1 dispersion, however, not all the involved model parameters could be determined reliably. Additional data on the angular dependence allow improvement of the model analysis.

In field-cycling experiments, where the external Zeeman fields B_0 and B_Δ can become of the order of the internal dipolar local field B_{loc} of the spins, the overall observable relaxation time T_1 becomes in extension of equation (4) a weighted mixture of the Zeeman [21] and Jeener's **d**ipolar [4] relaxation times T_{1Z} and T_{1D}, which according to Goldman [22] should follow the expression

$$T_1^{-1} \equiv R_1 = \frac{B_\Delta^2/T_{1Z}(\nu, \Delta) + B_{loc}^2/T_{1D}(\nu, \Delta)}{B_\Delta^2 + B_{loc}^2}, \quad (7a)$$

with

$$\nu \cong \frac{\gamma}{2\pi}((B_z + B_{loc})^2 + B_x^2)^{1/2}. \quad (7b)$$

Neither the spectral densities for T_{1D} are available in the literature to the same extent as for T_{1Z}, nor does there exist a critical experimental examination of the validity of equation (7), but approximate predictions about T_{1D} give in the spin-pair $I = 1$ approximation [23]

$$T_{1D}^{-1}(\nu, \Delta) \equiv R_{1D} = \sum_M R'_{1M} \quad (8a)$$

with

$$R'_{1M}(\nu, \Delta) = \frac{27}{8}\left(\frac{\mu_0 \gamma^2 \hbar}{4\pi}\right)^2 J_M^{(1)}(\nu, \Delta), \quad (8b)$$

using the same notation as for T_{1Z}. If $B_{loc} \ll B_0$, the dipolar contribution to the total relaxation rate $1/T_1 = R_1$ in equation (7) becomes negligibly small.

The *order fluctuation* terms $J_{OF}^{(q)}(p\nu)$ with explicit model parameters A, ν_{CL}, ν_{CH}, equations (9 *a*, 9 *b*), show the characteristic square-root law [24] of the order fluctuation spectral density $J_{OF}^{(1)}(\nu)$, where the amplitude A, equation (9 *a*), is molecule dependent, and predict $J_{OF}^{(2)}(\nu) = 0$, equation (9 *a*). This has been confirmed by many previous $T_1(\nu)$ studies [5, 6]; however the high and low cut-off frequencies ν_{CH} and ν_{CL} in equation (9 *b*) or the related mode wavelengths could not be determined satisfactorily because of the difficult separation of the T_{1OF} from other competing relaxation contributions, in particular from local field effects. The angular dependences expected by equations (4, 6), e.g. $T_{1OF}(\nu, 0°)/T_{1OF}(\nu, 90°) = 2{\cdot}5$ for $\nu < \nu_{CL}$ and $T_{1OF}(\nu, 0°)/T_{1OF}(\nu, 90°) = 1{\cdot}9$ for $\nu > \nu_{CL}$, become quite different when local fields determine the relaxation profile and the approximations involved by equations (7, 8) no longer hold. In this case the ratio $T_{1OF}(0°)/T_{1OF}(45°)$ can become very large (up to 6) due to potential contributions of the $J^{(0)}$ spectral density, and even a $T_1(\nu, \Delta)$ minimum may occur with decreasing Larmor frequency ν or changing angle Δ, respectively. Therefore the T_{1Z}/T_{1D} ratio at the minimum positions provide critical checks of the underlying relaxation model, in particular about the applicability of equation (8 *b*).

The *rotational diffusion* terms $J_{ROT}^{(q)}(p\nu)$ with explicit model parameters τ_{ROT} and σ, equations (10 *a*–10 *c*), discussed in the literature for deuteron NMR-studies have different forms. They essentially try to distinguish four types of rotational reorientations effective for the relaxation rates, namely: (i) the simple Woessner [21, 26] approach of rotating ellipsoids; (ii) the rotational *small-step* diffusion in an orienting potential (Nordio [27], Brown [28]; (iii) the anisotropic viscosity model (Freed [20]) in combination with fast spinning around the molecular long axis (Vold [29]), the so called *third rate* model; and (iv) extensions of (ii) or (iii) which include correlated, uncoupled chain mobilities (Dong [3, 30, 31]). Because of only small differences, so far an unambiguous experimental distinction between the two basically different approaches, i.e. Nordio's *small step* rotational diffusion (ii) and Vold's *third rate* model (iii), could not be achieved, but preferences are given to the extended third rate model [3, 31].

In the Appendix, the spectral densities have been split into the chain spin positions (N_{chain}) and the ring spin positions (N_{ring}) for convenience, equation (10 *a*). Equations (10 *b*, 10 *c*) show the averaging over the proton positions (sum over i, j) and the spectrum of rotational correlation times (sum over h). The inclusion of the chain mobility contains the sum over n, the number of the eigenvalues λ_n of the rate matrix corresponding to the number of chain conformations. The amplitude factors in equations (10 *b*, 10 *c*, 10 *g*), namely $C_{qm}^{(h)}(i,j)$, $C_{qmn}^{(h)}(i,j)$, and $C_m(i,j)$, are determined by the molecular geometry. The main differences between Nordio's [27] and Vold's [29] models occur in the definition and the summation over the basic correlation times τ_{qm}, equations (10 *d*, 10 *e*). In the first case the τ_{qm} values are related to the rotational diffusivities $D_{R\perp}$ and $D_{R\parallel}$ perpendicular or parallel to the molecular long axis, and in the second case to the diffusion constants D_α, D_β and D_γ, where α, β and γ refer to the Euler angles between the director and the molecular frame [29, 31]. The distinctions modify the ratios of the spectral densities $J_{rot}^{(1)}$ and $J_{rot}^{(2)}$ and thus finally lead to changes of the angular dependences of the relaxation times for a given anisotropy ratio σ_{Nordio}

$= D_{R\parallel}/D_{R\perp}$ or $\sigma_{\text{Vold}} = D_\alpha/D_\beta$, respectively. At low Larmor frequencies (extreme narrowing limit) $T_1(0°)/T_1(90°)$ can become rather high in Vold's model, namely for, e.g. $\sigma > 10$ larger than 3 instead of a maximum of 2 (neglecting chain motions) for Nordio's model, where the relaxation anisotropy is almost independent of σ. Therefore it is in principle easy to find a preference between the disputed models, if the measured anisotropy becomes larger than 2, in spite of the drawbacks due to the averaged proton spin signal, compared with deuteron studies.

The *translational diffusion* terms $J^{(q)}_{\text{SD}}(pv, \Delta)$ with the explicit model parameters B, τ_{SD}, ε, equations (11 *a*, 11 *b*), calculated by Vilfan and Žumer [32] for nematic LCs are not strongly different from the simple Pfeifer-Abragam [21] treatment of isotropic liquids, but bring into play a small, yet very characteristic angular dependence $T_{1\text{SD}}(\nu, 0°)/T_{1\text{SD}}(\nu, 90°)$. According to equation (11 *a*) this ratio depends mainly on the anisotropy $\varepsilon = D\parallel/D\perp$ of the diffusion constants $D_\parallel$ and $D_\perp$ for translational motion parallel and perpendicular to the director. It is nearly constant as a function of ν for jumping times τ_{SD} in the limit $2\pi\nu\tau_{\text{SD}} \leqslant 1$; in this case with ε between 1 to 3, it varies from 0·94 to 0·73. For a typical experimental result of $\varepsilon = 2$, it can be approximated by 0·8 [33] over the whole available Larmor frequency range from 0 to 100 MHz. The most pronounced feature of the Vilfan-Žumer SD-model is the fact that the predicted ratio $T_{1\text{SD}}(0°)/T_{1\text{SD}}(90°)$ is *smaller than one* in contrast to $T_{1\text{rot}}(0°)/T_{1\text{rot}}(90°)$, which in the same limit is *equal to or larger than two*. So the angular dependence of T_1 in principle becomes a sensitive tool to separate intermolecular from intramolecular relaxation contributions [34].

4.2. *Discussion*

The measured longitudinal relaxation times $T_1(\nu, \Delta)$ were fitted to the model expressions $T_1(\nu, \Delta)$ listed in the Appendix by a standard Levenberg-Marquardt least-square optimization procedure (Micromath Scientist) of the 8 model-parameters (A, ν_{CL}, ν_{CH}; τ_{ROT}, σ; B, τ_{SD}, and B_{loc}). Table 1 summarizes the best set obtained under the additional constraint that the same parameters should fit both the $T_1(\nu, \Delta = 0°)$ data and the $T_1(\nu, \Delta = 90°)$ data with the same quality. This constraint improves the reliability of the obtained parameters considerably. Even the limited 8CB $T_1(\nu, \Delta = 90°)$ data up to only $\nu = 4{\cdot}6$ MHz allow one to separate reliably the inter- from the intramolecular motions by using the theoretically predicted angular dependences. Additional curve fits were produced using on the one hand calculated values of the Cs (see § 4.2.2), and on the other hand experimental data for B_{loc} [35]; the cut-off frequency ν_{CH} was generally estimated from the shortest OF-mode determined by the molecular length. In this way the number of adjustable constants could be reduced from 8 to 5. Analysing typically about 30 Larmor frequencies, the underlying data sets make use of up to 50 data points at constant temperature.

The quality of a model fit to the experimental $^1\text{H} - T_1(\nu, \Delta)$ data is illustrated for 5CB at two orientations, i.e. $\Delta = 0°$ and $\Delta = 90°$, by figure 6. It is obvious from the experimental relaxation times shown in figure 4 that the related analysis of 8CB cannot lead to significant distinctions. The results support our previous work [6] at $\Delta = 0°$ where it was found that the collective motions dominate the T_1 relaxation dispersion at low νs up to about 500 kHz, and the importance of the individual molecular motions increases at higher νs. But the new data reveal many more details; they are explained below.

4.2.1. *OF-term*

Due to the broad T_1 square-root regime in the kHz range, the obviously dominating relaxation by order director fluctuation can be fitted rather precisely to the experimental data with a standard deviation for the normalized amplitude $A_{\text{OF}} \equiv A \cdot Z$ of about $\pm 10\%$, where the factor

$$Z = \frac{9}{8}\left(\frac{\mu_0 \gamma^2 \hbar}{4\pi}\right)^2 = 6{\cdot}408 \cdot 10^{-49}\,\frac{m^6}{s^2} \qquad (12\,a)$$

Table 1. Relaxation model parameters obtained by the Levenberg-Marquard fit optimization for 5CB and 8CB. Obviously both data sets are rather similar, which demonstrates that the fitting process is reliable and reproducible. Based on the experimental findings of Boden *et al.* [40] that the second moments of 5CB and 8CB chain protons are identical within 5%, we used the $C^{(h)}_{qmn}$s calculated for 5CB also to optimize the rotational parameters τ_{rot} and σ of 8CB. The σ value in the case of Nordio's model was taken from the literature [30] because in this work a critical evaluation proved impossible.

		Equation	5CB ($T = 30$°C)	8CB ($T = 37$°C)
$A_{\text{OF}}(\text{s}^{3/2})$		(9 *a*)	4635 ± 125	4806 ± 144
ν_{CL}(Hz)		(9 *b*)	< 2400	< 2100
$\tau_{\text{ROT}}(10^{-9}\text{s})$	Vold	(10 *e*)	3·3 ± 0·17	2·8 ± 0·2
	Nordio	(10 *d*)	2·17 ± 0·12	1·9 ± 0·11
σ	Vold	(10 *e*)	2·9 ± 0·3	2·9 ± 0·8
	Nordio	(10 *d*)	30	30
$D_\gamma(10^8\text{s}^{-1})$		(10 *f*)	> 5	> 6
$B_{\text{SD}}(10^8\text{s}^{-2})$		(11 *a*)	3·8 ± 0·9	4·2 ± 1·1
$\tau_{\text{SD}}(10^{-10}\text{s})$		(11 *b*)	3·65 ± 0·45	5·7 ± 0·78
$B_{\text{LOC}}(10^{-5}\text{T})$		(7 *a*)	6 ± 3·3	5 ± 1·9
$a_0(\text{s}^{-1})$		(14)	383 ± 65	383 ± 20
$a_1(\text{s}^{-1})$		(14)	428 ± 73	121 ± 12
$a_2(\text{s}^{-1})$		(14)	−417 ± 71	−431 ± 42

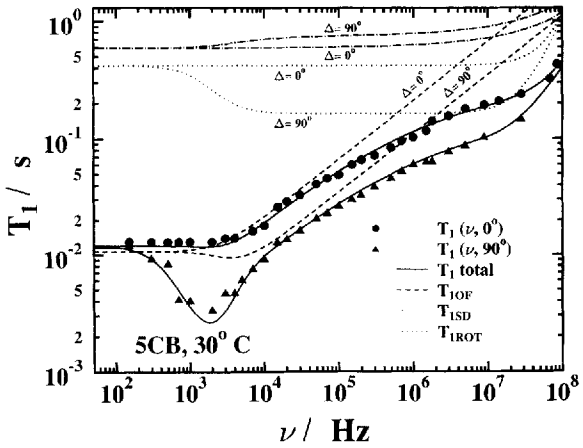

Figure 6. $T_1(\nu, 0°)$ and $T_1(\nu, 90°)$ model fits (full lines) of equations (3-9, 10*a*-10*c*, 10*e*, 11, 13 and 14) to the 5CB measurements (circles and triangles) of figure 4 with model parameters listed in table 2. The six broken lines show the individual relaxation contributions by order fluctuations, self-diffusion and rotational diffusion.

is included for convenience, e.g. for 5CB at 30°C we obtain $A_{OF} = 4671 \pm 400\, s^{3/2}$. Taking into account simultaneously the observed angular dependence over the square-root regime, gives in this case a reduced standard deviation of only ±5%, namely $A_{OF} = 4635 \pm 125\, s^{3/2}$; both values are slightly smaller than our previous result [6]. These numbers have to be compared with the theoretical expression [6]

$$A_{OF} = \frac{\pi^{1/2}}{2} \langle \Delta\nu \rangle^2 \frac{k_B T \eta^{1/2}}{K^{3/2}} \qquad (12\,b)$$

and known data for the mean elastic constant K(1·52 $\times 10^{-11}$ N ± 15% at 30°C) [36], mean viscosity η (0·043 Pas ± 10% at 30°C) [37], and mean experimental splitting $\langle \Delta\nu \rangle$ of the 5CB proton spectrum, which was determined from the FID signal as 17360 Hz ± 10% consistent with data from the literature [35] and our own data. From equation (12) there follows $A_{OF} = 3911 \pm 1200\, s^{3/2}$, a value in good agreement with the relaxation measurements within the error limits.

In spite of the higher temperature of the nematic 8CB phase, the measured value of A_{OF} is somewhat larger than for 5CB, namely $A_{OF} = 4806 \pm 144$ at 37°C. But again the result is in good agreement with the theoretical prediction by equation (12), namely $A_{OF} = 4440 \pm 1470\, s^{3/2}$, using $K = 1{\cdot}6 \times 10^{-11} N \pm 15\%$ [36], $\eta = 0{\cdot}045$ Pas [37] and $\langle \Delta\nu \rangle = 18800$ Hz ± 10%. Since one should assume that the error limits for the *ratios* of the various parameters are smaller than for the *absolute* T_1, K, η and $\langle \nu \rangle$ measurements, the observed ratio $A_{OF}(5CB)/A_{OF}(8CB) = 0{\cdot}96$ allows a more critical examination of the theory. The respective ratio calculated by equation (12) is 0·97. This demonstrates once more, that the T_{1OF} concept is basically correct.

Whereas the low frequency plateau in the relaxation dispersion at $\Delta = 0°$ can be interpreted either by assuming a longest cut-off mode via equation (9*b*) or a local field effect via equation (7*a*), the new data for $\Delta = 90°$ clearly reveal that the second effect dominates, considering the following argument: a finite local field B_{loc} along the z-axis [38] entails locally an effective angle Δ_{eff} between the director **n** along the z-axis and the resulting field $\mathbf{B}_\Delta$ different from Δ in equation (1), namely

$$\Delta_{eff} = \arctan\left(\frac{B_x}{B_z + B_{loc}}\right), \qquad (13)$$

which means that for B_z comparable or smaller than B_{loc} the angle Δ_{eff} becomes smaller than the externally adjusted angle Δ (e.g. 90°) between **n** and $\mathbf{B}_\Delta$. In our calculation of the angular dependence, Δ_{eff} was used throughout even where the local field effect is completely negligible. As seen in figure 4, $T_1(\nu)$ runs through a minimum near $B_z \cong B_{loc}$ since with decreasing $\nu = \gamma B_\Delta$ the angle Δ_{eff} also necessarily decreases and thus finally $T_1(\nu, \Delta = 90°)$ approaches $T_1(\nu, \Delta = 0°)$. However, the observed low field behaviour is only in qualitative agreement with this concept on the basis of equations (7, 8) because the experimental $T_{1OF}(\nu, \Delta = 0°)/T_{1OF}(\nu, \Delta = 90°)$ ratio considerably exceeds the maximum value of 2·6 predicted by equations (6*a*, 6*b*; 9*a*, 9*b*) in the case of $\nu_{CL} > \gamma B_{loc}/2\pi$. This implies that the common approximation of T_{1D} by equations (8*a*, 8*b*) cannot be valid. A possibility of producing a stronger angular dependence in the OF-model can be achieved by including the spectral density $J^{(0)}_{OF}(\nu, \Delta)$ and $J^{(2)}_{OF}(\nu, \Delta)$ in addition to $J^{(1)}_{OF}(\nu, \Delta)$, in the T_{1D} term. Using in replacement of equations (8*a*, 8*b*) the generalized expression given by Morrison *et al.* [7]

$$T_{1D}^{-1} = a_0 + a_1/P_2(\cos(\Delta_{eff})) + a_2/P_4(\cos(\Delta_{eff})), \qquad (14)$$

where a_0, a_1 and a_2 are adjustable model parameters and P_2 and P_4 are the Legendre polynomials of 2nd and 4th order, it becomes possible to describe the form of the observed $T_1(\nu)$ minimum much better. But in this case the B_{loc} value involved in equations (7, 13, 14) for the *best fit* shown in figure 4 turns out considerably too small ($B_{loc} \cdot \gamma/(2\pi) = 2400$ Hz) relative to estimations from the high-field proton spectrum ($B_{loc} \cdot \gamma/(2\pi) = 17360$ Hz). This could indicate that the slowest, large amplitude order fluctuations partially average the dipolar field. Alternative model optimizations obtainable with higher B_{loc} values and by means of the simpler T_{1D} relation [23], equation (8*b*), in replacement of equation (14) are illustrated in figure 7. All resulting curve parameters considered in the relaxation plots for both materials are summarized in table 2.

As a consequence of the strong local field effect, the low cut-off frequency ν_{CL}, attributed previously as a rule to the low-field plateau, can no longer be evaluated exactly. But the dominating local field effect in the kHz regime requires, in order to obtain the $T_1(\nu, \Delta)$ minimum, that ν_{CL} should be smaller than $\gamma B_{loc}/2\pi$, i.e. approximately 2·5 kHz for both materials. Similarly, the high cut-off frequency ν_{CH} is almost hidden within the experimental error limits by the two other relaxation contributions T_{1ROT} and T_{1SD}. Nevertheless, assuming that the square-root dispersion profile for T_{1OF} is valid at least up to frequencies where the T_{1OF} contribution amounts to still 30% of the total T_1 value, on the one hand the *lower* limit of ν_{CH} should be larger than 30 MHz for 5CB and 10 MHz for 8CB, respectively. On the other hand, using the results for the rotational correlation time $\tau_{ROT} = (6D_{R\perp})^{-1}$ (see §4.2.2), the *upper* limit of ν_{CH} should not exceed $(2\pi\tau_{ROT})^{-1}$, the frequency where individual reorientations about the short axis are faster than the collective ones; this gives limits of approximately 40 and 60 MHz.

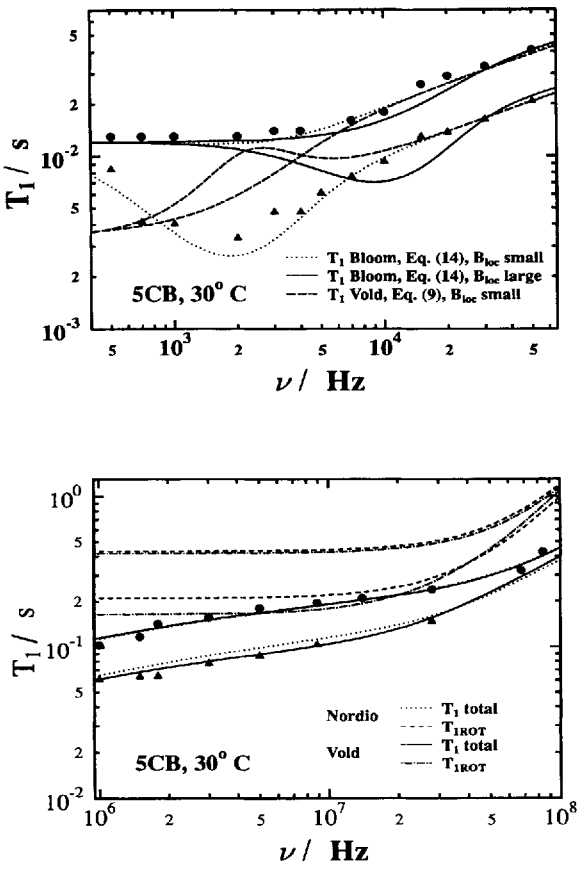

Figure 7. Enlarged view of the low- and high-frequency ranges of the 5CB data with alternative model curves. Top: low frequency measurements from figure 6 with the best model fit (dotted line) as in figure 6; a simulation (full line) using equations (7, 14) with a stronger local field ($\equiv \nu_{loc} = 14$ kHz in replacement of 2·4 kHz); and a simulation (broken line) using equation (8) in replacement of equation (14). Bottom: high frequency measurements with fits from figure 6 and fits using Nordio's model (dotted line, equation (10*d*)) in replacement of Vold's model (full line, equation (10*e*)) to demonstrate the preference of the Vold approach, where the standard fit deviation Σ is smaller by a factor of approximately 0·8.

4.2.2. *ROT- and SD-term*

The disentanglement of the rotational and translational diffusion relaxation terms from the total $T_1(\nu, \Delta)$ is less straightforward than the analysis of the order fluctuation contribution, because there exists no frequency range where $T_1(\nu)$ is unambiguously dominated by a characteristic power law of either T_{1ROT} or T_{1SD}. However, the rather strong angular dependence at Larmor frequencies $\nu \geqslant 10$ MHz, where the T_{1OF}-term no longer governs the dispersion profile, indicates not only that the rotational relaxation term is more effective than the other two processes, but also shows that Vold's model, equations (10*a*–10*c*, 10*e*, 10*f*), is more appropriate than Nordio's concept, equations (10*a*–10*d*, 10*f*). To calculate the curve fits shown for 5CB in figure 4, and similar plots for 8CB not shown, we proceeded in the following way.

First, the rotational quantities $C_{qm}^{(h)}$, $b_{qm}^{(h)}$ and C_m ($q = 0, 1, 2$; $m = 0, 1, 2$) were calculated numerically from the molecular geometries with the formalism of Woessner [26] and Vold *et al.* [29], respectively, using the proton pair separations $r_{CH_2} = 1{\cdot}78 \cdot 10^{-10}$ m, $r_{C_6H_6} = 2{\cdot}48 \cdot 10^{-10}$ m, the polar angles φ and ϕ of the CH_2 pair-orientations in the tetrahedral lattice frames (a, b, c, d; a', b', c', d') according to Wittebort *et al.* [39], and the C_6H_6 *para*-pairs parallel to the molecular long axis. These angles are listed in table 2. For simplicity intra-pair interactions were taken into account on the basis of Boden's experimental finding for 5CB and 8CB [40] that the ratio between dipolar inter-pair and intra-pair interactions is close to one. The amplitudes $C_{qmn}^{(h)}$ ($n = 1$ to 51) and eigen values $\lambda_n(k)$, which take into account the chain mobility, were calculated following Dong [30, 41], assuming that the one- and two-bond jumps have an equal rate constant k and neglecting the effect of three-bond jumps (as in Dong's paper [41]). With this simplifying assumption, the eigen values $\lambda_n(k)$ are proportional to k. *Then*, with the calculated quantities and previous experimental results on the translational diffusion process [33], i.e. for $D_\perp$ and the diffusion anisotropy $\varepsilon = D_\parallel / D_\perp$, model simulations and curve fits were performed by means of the Levenberg–Marquardt procedure [42]; such steps allowed optimization of the *rotational* correlation time τ_{ROT} of the model, the underlying rotational anisotropy σ, and the open *translational* parameters B and τ_{SD}. Fitting D_γ (related to three $K_{\gamma m}$s

Table 2. Ch_2 group polar angles (θ, φ) of the proton-proton separation vectors in the n-CB chain configuration frame (N-frame) calculated from the basis vectors for the alcyl chain (tetrahedral) lattice in both the unprimed, right handed (**a**, **b**, **c**, **d**) and the primed, left handed (**a'**, **b'**, **c'**, **d'**) system following the notation of Wittebort *et al.* [39].

Spin spin vector	θ	φ
a-b	35·25°	60°
a-c	35·25°	180°
a-d	35·25°	−60°
b-c	90°	−150°
b-d	90°	−90°
c-d	90°	150°
a'-b'	144·75°	−120°
a'-c'	144·75°	0°
a'-d'	144·75°	120°
b'-c'	90°	30°
b'-d'	90°	90°
c'-d'	90°	150°

of Vold's model), and the isomerization rate constant k of the considered two types of correlated chain jumps did not work satisfactorily because of the too small effects on $T_1(\nu)$. But the explicit dependence of the rotational jump times τ_{qm} on the third rate process parameter $K_{\gamma m}$, and of the spectral density on k makes it possible to determine the slowest limits of the γ-motion and of the chain isomerization rate k, where a further slowing down considerably deteriorates the fit. Essentially due to the proportionality between λ_n and k, the low-frequency T_1 plateau reflects the values of both the $K_{\gamma m}$s and k, and this dependence is responsible for the good agreement between the calculated and fitted spectral densities in the limit of $\nu \to 0$. To separate both effects, the value of D_γ was estimated using the results of τ_{ROT} and σ in the approximation that $D_\gamma \cong D_{R\parallel}$, $D_\beta \cong D_{R\perp}$.

Similarly to the treatment of the OF-term, B was normalized by multiplication with Z from equation (12 a) to $B_{SD} \equiv B \cdot Z$. All steps were repeatd for the competing rotational concepts, and *finally* the results were analysed in terms of the obtained fit qualities for the Nordio, Vold and Woessner models, respectively. Table 1 lists the evaluated best model parameters.

The involved standard deviations Σ between suitably weighted calculated and observed data [42] allow rather clear conclusions about the effective type of rotational process because the Σs are different for the two favoured alternative models, namely by a factor of 1·2 ($\Sigma_{Vold} = 0{\cdot}014$; $\Sigma_{Nordio} = 0{\cdot}017$) when comparing the result of equation (10 d) with that of equation (10 e). Woessner's approximation can be easily excluded without a detailed calculation, because of the absent anisotropy. Nevertheless it should be noted, that the calculated C_m amplitudes are in satisfactory agreement with the measurements, in particular the summations for the longer chains of 8CB compared with 5CB result in an increase of the Woessner contribution to the overall relaxation rate by a maximum of 5% in accordance with the experimental findings. As demonstrated by figure 7 for 5CB, Vold's third rate model [29] allows the best interpretation of the measurements, mainly due to the rather large relaxation time anisotropy above $\nu \cong 500$ kHz, whereas Nordio's expression does not fit the $T_1(\nu, \Delta)$ data between $\nu = 1$ MHz and 20 MHz with the same quality. This conclusion improves Dong's analysis by deuteron relaxation studies [30, 41], which for 5CB failed to give a clear preference for one of the two concepts.

The reorientation time $\tau_{ROT} \approx (2{\cdot}5 \pm 0{\cdot}4) \cdot 10^{-9}$ s and the rate constant $k \approx (4 \pm 2) \times 10^{11}\ s^{-1}$ determined by our study are almost identical with Dong's findings for 5CB, whereas the anisotropy parameter σ based on Vold's concept turns out much larger (2·9) than Dong's results (1·8) in this case. This difference is essentially the consequence of the importance of the OF-team to the overall relaxation in the high-field regime which was neglected in the deuteron study. It should be noted that in the present case neither the order fluctuation contribution nor the translational self-diffusion term entail a significant uncertainty of the fitting procedure, because the related parameters A_{OF} and ε are rather exactly determined by the performed experiments.

Dong's more recent refinements [43] of Nordio's theory, by taking into account the coupling between reorientations of the chain and of the whole molecule, have not been treated in this work because of the too small changes of the proton spectral densities. Furthermore, the interesting behaviour of τ_{ROT} at the transition from the nematic to the isotropic phase (35·3 ± 0·2)°C could not be evaluated more critically than in previous work because of the vanishing angular dependence of T_1. However, simple estimates by means of the isotropic Woessner model, equation (10 g), indicate that the dominant rotational correlation time, i.e. for diffusion about the short axis, becomes shorter by a factor of about two.

The authors thank Dipl. Phys. H. Gotzig for frequent experimental help, I. Sauter and St. Köhle for their contributions to the development of the saddle coil, and Professor H. Schmiedel for preparing the 5CB anopore sample. The financial support of this work by Professor G. Klose, Sonderforschungsbereich 294 Leipzig, and by the Deutsche Forschungs Gemeinschaft, is gratefully acknowledged.

Appendix

Spectral densities $J_M^{(q)}(p\nu)$ used in the model fitting procedure to the T_1 measurements of figures 4–7. The amplitudes (A, B), correlation times (τ_{ROT}, τ_{SD}), mode

cut-off frequencies (ν_{CH} and ν_{CL}), and further specific model parameters (σ, ε and α) are defined in the references given in the text. $N = N_{Ring} + N_{Chain}$ are the respective numbers of protons per molecule, e.g. for 5CB $N_{Ring} = 8$, $N_{Chain} = 11$. In the case of 5CB the number of eigen values is $n_{max} = 51$. The prefactors f_q are $f_0 = 6$, $f_1 = 1$, and $f_2 = 4$ [21]. Since the Woessner model was derived for an isotropic fluid, $J_{ROT}{}^{(q)}$ of equation (10 *g*) is valid for any angle Δ, in particular for $\Delta = 0$. In this case, the angular dependence by the factors of equations (6 *a*, 6 *b*) also disappears [28].

Order fluctuation terms [24, 25]:

$$J_{OF}^{(1)}(pv) = \frac{A}{(pv)^{1/2}}\left[1 - G_{CL}(\nu/\nu_{CL}) - G_{CH}(\nu/\nu_{CH})\right],$$

$$J^{(2)}(pv) = 0,\ J^{(0)}(pv) = 0; \tag{9 a}$$

with

$$G_{CL} = -\frac{1}{\pi}\left\{a\tan\left[\frac{(2pv/\nu_{CL})^{1/2}}{(1 - pv/\nu_{CL})}\right] + a\tanh\left[\frac{(2pv/\nu_{CL})^{1/2}}{(1 + pv/\nu_{CL})}\right]\right\} + \delta, \tag{9 b}$$

$$G_{CH} = \frac{1}{\pi}\left\{a\tan\left[\frac{(2pv/\nu_{CH})^{1/2}}{(1 - pv/\nu_{CH})}\right] + a\tanh\left[\frac{(2pv/\nu_{CH})^{1/2}}{(1 + pv/\nu_{CH})}\right]\right\} + \delta, \tag{9 c}$$

and

$$\left.\begin{array}{l}\delta = 1 \quad \text{for } pv < \nu_{CL}\\ \rho = 1 \quad \text{for } pv > \nu_{CH}\end{array}\right\} \text{else } 0.$$

Rotational diffusion terms [3, 27–30]:

For Nordio's and Vold's models

$$J_{ROR}^{(q)}(pv) = J(pv)_{Ring}^{(q)} + J(pv)_{(Chain)}^{(q)},\quad q = 0, 1, 2; \tag{10 a}$$

with

$$J^{(q)}(pv)_{Ring} = f_q \frac{1}{N}\sum_{i<j}^{N_{Ring}}\sum_{m=0}^{2} \cdot \sum_{h=1}^{3} C_{qm}^{(h)}(i,j)\,\frac{\tau_{qm}^{-1(h)}}{(2\pi pv)^2 + (\tau_{qm}^{-1(h)})^2}, \tag{10 b}$$

$$J^{(q)}(pv)_{Chain} = f_q \frac{1}{N}\sum_{i<j}^{N_{Chain}}\sum_{m=0}^{2}\sum_{n=1}^{n_{max}}\sum_{h=1}^{3} C_{qmn}^{(h)}(i,j) \cdot \frac{\tau_{qm}^{-1(h)} + |\lambda_n(k)|}{(2\pi pv)^2 + (\tau_{qm}^{-1(h)} + |\lambda_n(k)|)^2}, \tag{10 c}$$

and

$$\tau_{qm}^{(h)} = b_{qm}^{(h)}\tau_m,\quad \tau_m^{-1} = (6\tau_{ROT})^{-1}[6 + m^2(\sigma - 1)]$$

(Nordio [27]), (10 *d*)

$$\tau_{qm}^{-1(h)} = (b_{qm}^{(h)}\tau_q)^{-1} + K_{\gamma m},$$

$$\tau_q^{-1} = (6\cdot\tau_{ROT})^{-1}[6 + q^2(\sigma - 1)]$$

(Vold [29]), (10 *e*)

where

$$\tau_{ROT} = (6D_\perp)^{-1},\quad \sigma \equiv D_{R\parallel}/D_{R\perp},$$

$$K_{\gamma 0} = 0,\quad K_{\gamma 1} = D_\gamma,\quad K_{\gamma 2} = 4D_\gamma. \tag{10 f}$$

For Woessner's isotropic model [26]

$$J_{ROT}^{(q)}(pv) = f_q \cdot \frac{1}{N}\cdot\sum_{i<j}^{N} \cdot \sum_{m=0}^{2} C_m(i,j)\,\frac{\tau_m}{1 + (2\pi pv\tau_m)^2}. \tag{10 g}$$

where

$$\tau_m^{-1} = (6\tau_{ROT})^{-1}[6 + m^2(\sigma - 1)],\quad \sigma \equiv D_{R\parallel}/D_{R\perp}. \tag{10 h}$$

Translational self-diffusion terms [32]:

$$J_{SD}^{(q)}(pv) = B\cdot\tau_{SD}\cdot j^{(q)}(pv, \tau_{SD}, \varepsilon, \alpha), \tag{11 a}$$

where

$$\tau_{SD} = \frac{\alpha d^2}{D_\perp},\quad \varepsilon = \frac{D_\parallel}{D_\perp},\quad \alpha = \frac{\langle r_\perp^2\rangle}{d^2}. \tag{11 b}$$

Note added in proof

After submission of this paper, R. Y. Dong (private communication, 1996) reported errors in the original papers for equations (10 *d*) and (10 *e*), which change the definition of the correlation times $\tau_{qm}^{(h)}$ of Nordio's and Vold's model. As a consequence the factor $(\sigma - 1)$ in both equations must be multiplied with $b_{qm}^{(h)}$, in addition to the $b_{qm}^{(h)}$ dependence of the equations used in the Appendix. As the factors $b_{qm}^{(h)}$ are smaller than 1, the anisotropy ratio σ has less influence on the correlation time τ_{ROT} than before. However, this leads to only minor corrections of the τ_{ROT} model fit data listed in table 2, namely, e.g. for 5CB from 3·30 ns to 3·31 ns (Vold) and from 2·17 ns to 2·11 ns (Nordio). The correction of σ is larger, namely from 2·9 to 4·4.

Evidently these results do not change our conclusion about the preference of Vold's model; more than that

with the corrected formulae the preference becomes slightly better.

References

[1] *Nuclear Magnetic Resonance of Liquid Crystals*, 1985, edited by J. W. Emsley (Dordrecht: D. Reidel).

[2] *The Molecular Physics of Liquid Crystals*, 1994, edited by G. R. Luckhurst and C. A. Veracini (Dordrecht: D. Reidel).

[3] DONG, R. Y., 1994, *Nuclear Magnetic Resonance of Liquid Crystals* (Heidelberg: Springer).

[4] JENNER, J., and BROEKAERT, P., 1967, *Phys. Rev.*, **157,** 232.

[5] NOACK, F., NOTTER, M., and WEISS, W., 1988, *Liq. Cryst.*, **3,** 907.

[6] KÖLLNER, R., SCHWEIKERT, K. H., NOACK, F., and ZIMMERMANN, H., 1993, *Liq. Cryst.*, **13,** 483.

[7] MORRISON, C., and BLOOM, M., 1993, *J. magn. Res. A*, **103,** 1.

[8] GRAF, V., REINHART, K. F., NOACK, F., and STOHRER, M., 1976, in Proceedings of XIXth Congress Ampère, Heidelberg.

[9] WÖLFEL, W., 1978, thesis, University of Stuttgart, Germany.

[10] NOACK, F., 1986, *Prog. nucl. magn. Res. Spectrosc.*, **18,** 161.

[11] EMSLEY, J. W., LINDON, J. C., LUCKHURST, G. R., and SHAW, D., 1973, *Chem. Phys. Lett.*, **19,** 345.

[12] DOANE, J. W., TARR, C. E., and NICKERSON, M. A., 1974, *Phys. Rev. Lett.*, **33,** 620.

[13] GOTZIG, H., GRUNENBERG-HASSANEIN, S., and NOACK, F., 1994, *Z. Naturforsch.*, **49a,** 1179.

[14] ROMMEL, E., MISCHKER, K., OSSWALD, G., SCHWEIKERT, K.-H., and NOACK, F., 1986, *J. magn. Res.*, **70,** 219.

[15] BEYERLE, K., 1931, *Arch. Elektrotechnik*, **25,** 267.

[16] FUKUSHIMA, F., and ROEDER, S. B. W., 1991, *Experimental Pulse NMR* (London: Addison-Wesley), p. 386.

[17] CRAWFORD, G. P., VILFAN, M., DOANE, J. W., and VILFAN, I., 1991, *Phys. Rev. A*, **43,** 835.

[18] CRAWFORD, G. P., STANNARIUS, R., and DOANE, J. W., 1991, *Phys. Rev. A*, **44,** 2558.

[19] STRUPPE, J., and NOACK, F., 1994, Abstracts 15th ICLC, July (Budapest: REPS).

[20] FREED, J. H., 1977, *J. chem. Phys.*, **66,** 4183.

[21] ABRAGAM, A., 1970, *The Principle of Nuclear Magnetism* (Oxford: Clarendon Press), p. 297.

[22] GOLDMAN, M., 1970, *Spin Temperature and Nuclear Magnetic Resonance in Solids* (Oxford).

[23] VOLD, R. R., and VOLD, R. L., 1988, *J. chem. Phys.*, **88,** 4655.

[24] BLINC, R., HOGENBOOM, D., O'REILLY, D., and PETERSEN, E., 1969, *Phys. Rev. Lett.*, **23,** 969.

[25] GRAF, V. 1980, thesis, University of Stuttgart, Germany.

[26] WOESSNER, D., 1962, *J. chem. Phys.*, **37,** 647.

[27] NORDIO, P. L., RIGATTI, G., and SEGRE, U., 1972, *J. chem. Phys.*, **56,** 2117.

[28] BROWN, M. F., 1982, *J. chem. Phys.*, **77,** 1576.

[29] VOLD, R. R., and VOLD, R. L., 1988, *J. chem. Phys.*, **88,** 1443.

[30] DONG, R. Y., 1991, *Phys. Rev. A*, **43,** 4310.

[31] DONG, R. Y., FRIESEN, L., and RICHARDS, G. M., 1994, *Mol. Phys.*, **81,** 1017.

[32] VILFAN, M., and ŽUMER, S., 1978, *Phys. Rev. A*, **17,** 424.

[33] MAGER, J., 1993, thesis, University of Stuttgart, Germany.

[34] LEWIS, J. S., TOMCHUCK, E., and BOCK, E., 1987, *Can. J. Phys.*, **65,** 115.

[35] KOMOLKIN, A. V., LAAKSONEN, A., and MALINIAK, A., 1994, *J. chem. Phys.*, **101,** 4103.

[36] HAKEMI, H., JAGODZINSKI, E. F., and DUPRÉ, D. B., 1983, *J. chem. Phys.*, **78,** 1513.

[37] CHMIELEWSKI, A. G., 1986, *Mol. Crys. liq. Cryst.*, **132,** 339.

[38] THAYER, A. M., LUZAR, M., and PINES, A., 1987, *J. phys. Chem.*, **91,** 2194.

[39] WITTEBORT, R. J., and SZABO, A., 1978, *J. chem. Phys.*, **69,** 1722.

[40] BODEN, N., CLARK. L. D., CLARKE, C. G., and KAHOL, P. K., 1983, *Mol. Phys.*, **50,** 667.

[41] DONG, R. Y., and RICHARDS, G. M., *Mol. Crys. liq. Cryst.* (submitted).

[42] *Scientist Handbook*, Micro Math Inc., rev. 167BD, 1993 (Salt Lake City: Micro Math Inc.).

[43] DONG, R. Y., and RICHARDS, G. M., 1992, *Chem. Phys. Lett.*, **200,** 541.